

Received June 7, 2018, accepted July 15, 2018, date of publication August 10, 2018, date of current version September 7, 2018.

Digital Object Identifier 10.1109/ACCESS.2018.2864565

# Development of an Integrated Laser Sensors Based Measurement System for Large-Scale Components Automated Assembly Application

GAOLIANG PENG<sup>ID</sup>, (Member, IEEE), YU SUN, AND SHILONG XU

State Key Laboratory of Robotics and System, Harbin Institute of Technology, Harbin 150001, China

Corresponding author: Gaoliang Peng (pgl7782@hit.edu.cn)

This work was supported in part by Self-Planned Task, State Key Laboratory of Robotics and System (HIT), under Grant SKLRS201708A, and in part by the National High-Tech R&D Program of China (863 Program) under Grant 2015AA042201.

**ABSTRACT** In the field of precision docking or assembly of large scale, the orientation and position measurement system is quite demanding. This paper proposes a long-range measuring system with the combination of low-cost tilt sensor and laser sensors to achieve orientation and position deviation during the process of docking in the outdoor environment. The measuring principle and the system construction of the integrated system are introduced in detail. Subsequently, the geometric measurement model for each assembly stage is established. The measurement system is dividing the whole measuring process into six major alignment steps to complete the automated assembly task. Then, the proposed measuring system is applied to an automated antenna assembly system to demonstrate its effectiveness in large-scale measurement. Validation experiments were performed and the preliminary result shows that the proposed system could achieve high efficiency and accuracy for large volume components automated assembly. Our main contribution is developing a new orientation and position measuring method for 6-DOF automated assembly in the outdoor environment and proposing a new approach to reduce the errors in each direction based on the step-by-step adjustment, which provides a new idea for docking and assembly in complex environment.

**INDEX TERMS** Assembly systems, sensor systems, position measurement, large-scale systems.

## I. INTRODUCTION

Large components docking and assembly play an essential role in mechanical manufacturing industry such as aerospace, shipbuilding, and automobile industry [1]. To achieve the goal of automated assembling for large components, the most vital factors are adjustment mechanisms and measurement approach. Along with the applications of precise digital measurement technology and development of robotics, more advanced docking and assembly systems have emerged in the purpose of gains in productivity and cutting production cost.

In the field of large-scale metrology (LSM), researchers have devoted a lot and developed a large amount of apparatuses. With the development in optics, LSM technology has witnessed a rapid development in recent years [2]. Measurement devices like laser tracker [3], [4], computer aided theodolite (CAT), iGPS [5], [6] and optical based method [7], [8] have been widely used in large-scale measuring systems. Since 1990, commercial products such as

iGPS, gap gun, laser tracker, laser altimeter, etc. have emerged [9]–[12] and have been widely used in the fields of aerospace, scientific instruments and automotive industries. Take automated assembly of aircraft for example, firstly the precise location and pose of components are achieved by large-space digital measuring systems consisting of laser trackers or iGPS, then the control system gives signals to the pose adjusting mechanisms according to the pose and location information. This technology can improve the quality and efficiency of assembly of aircraft assembly [13], [14].

Some instruments based on optics have been put into commercial use. Optical measurement systems have advantages of long range, high resolution and strong to electromagnetic interference. Laser tracker have been proved to be able to get orientation and position with high accuracy over large range in real time [15], [16]. Xie *et al.* [17] developed a kind of eye-in-hand robot using laser pointer. Wang *et al.* [18] proposed an assembly system using laser sensors and other

vision-based sensors. Hsieh and Pan [19] developed a grating-based interferometer including three identical detection parts utilizing Michelson interferometry, heterodyne, and grating shearing. Chen *et al.* [20], [21] developed a laser straightness interferometer system to measure 6-DOF error parameters and considered simultaneously rotational error compensation. The greatest advantage of laser tracker is high accuracy. Nevertheless, the application is limited by its high cost.

The vision based method is also applicable in LSM and has been applied in the field of assembly line inspection and industry robots, etc. [22], [23]. The machine vision technology is able to help measure and locate three-dimensional objects. Some researchers have developed different measuring systems on the base of machine vision. Gao *et al.* [24] proposed a measurement system based on monocular vision and inclinometers. Similarly, Liu *et al.* [7] presented a system using stereo vision based 3D metrology technique to measure large-scale objects. Compared with other non-contact measuring methods, the cost of vision-based metrology is relatively lower. Though thousands of designs are based on computer vision, the method itself still has some problems that can't be ignored—most of the times, the accuracy and reliability can't meet the demands.

In addition to the methods mentioned above, there are also some other instruments and techniques in literature, such as laser scanning [25] and ultrasonic ranging [26]. Grosse-Schwiep M [27] used multiple synchronous laser scanners and cameras for determination of deformations of rotating rotor blades. However, there are still some problems remained. The sensors used may have a high accuracy, but the accuracy and reliability are unstable for large-scale components. Apart from limited accuracy, the high cost of these sensors is the foremost problem.

At the same time, most of the researches and experiments are designed for indoor environment. The influence of the environment is also a factor that restricts the application of these methods. Kim *et al.* [28] proposed a combination of low-cost sensors including infrared markers, three 1-D laser sensors, and vision cameras. This method is developed for a long-range motion-sensing system to navigate and track objects in maritime transportation. Meanwhile, 1-D sensor may also be able to realize the measurement of multi-DOF motion in a more economical way. Even though these systems have ability to get all orientation and position errors, the complex configurations, high cost, bulky size, and need for custom optics and complex targets are the significant shortcomings [29].

Therefore, we propose a novel low-cost measurement method to achieve high accuracy posture measurement for large-scale components assembly, such as aircraft, rocket or radar antenna, in outdoor environment. We installed tilt sensors and laser sensors at different positions in the mechanisms to measure the relative pose between the docking components, as to realize automated assembly process step by step. At the same time, we optimize the combination of

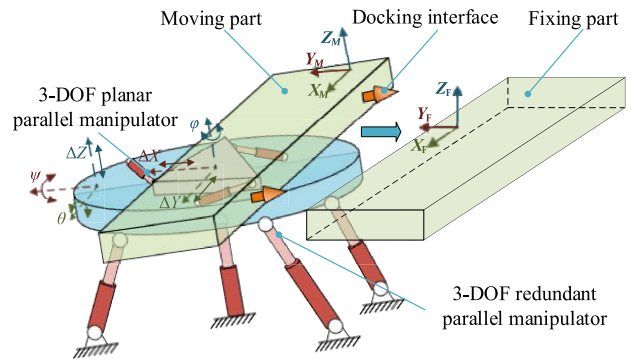


FIGURE 1. Overview of the docking system.

sensors with different measuring range and accuracy. This paper is structured as follows: section 2 outlines the system construction and measurement process of proposed method. Section 3 specifically establishes the geometric model of proposed measurement system. Then, an experiment is established to testify the measurement system and some discussion are made. In the end, section 5 demonstrates some concluding remarks and future work that needs to be done.

## II. A LARGE-SCALE MEASUREMENT SYSTEM CONSTRUCTION

For large-scale components automated assembly, it is necessary to get orientation and position of the moving part with respect to the fixed one by installing a measurement system. Since the distance between the two components may range from centimeters to meters, the system should keep an accuracy less than 1mm over such distance to guarantee proper adjustment. In addition, the system should guarantee a fault-free operation in outdoor environment.

In this section, we developed a long-range measurement system for a hybrid mechanism which consists of a 3-DOF redundant parallel manipulator and a 3-DOF planar parallel manipulator. As depicted in Fig. 1, the 3-DOF redundant parallel manipulator, with high stiffness, agility and payload capacity, is settled as the base which is able to accomplish pitching, rolling and translating along the Z axis. The 3-DOF planar manipulator, fixed on the redundant manipulator, is set to accomplish yawing and translating along X and Y axis.

The system aims to obtain the orientation and position information using a set of sensors including two tilt sensors, three photoelectric switch sensors (PSS), two 1-D laser range finders (LRF) and two position sensitive device (PSD)

sensors. As is shown in Fig. 2, the tilt sensors are set to get angular errors by X and Y axis, and then the mechanism adjust components to the horizontal plane independently. The photoelectric switch sensors (PSS), relatively low-cost distance sensors, are used to eliminate displacement errors roughly in Y and Z axis. The LRFs are used to measure the displacement errors between the two components in X axis, and then calculate the angular errors by Z axis.

the accuracy achievable.

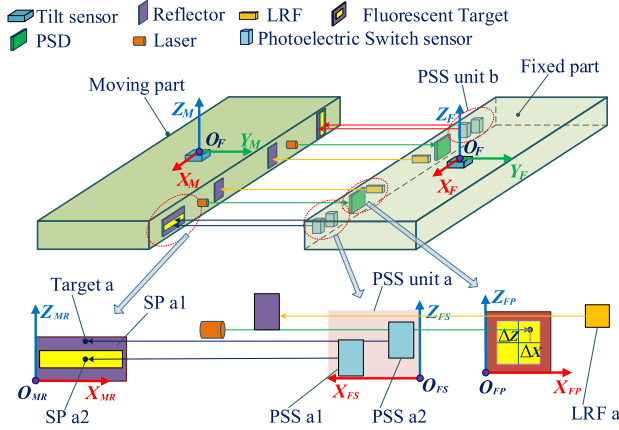


FIGURE 2. Overview of the measurement system.

Two PSSs are integrated into a range-finder unit for searching the target with a reflector. As illustrated in Fig. 2, from the projection view of sensors mounted face, the two beam focal spots will reach the target. If spot a1 is on the reflective stripe and spot a2 is not, it means the edge of reflective stripe is just between the two spots. In this state, the return value of PSS a1 is on and PSS a2 is off respectively, since PSS only works when its spot is on the reflective area. In the proposed system, PSS unit and unit b are set to narrow the errors along Z and X axis. The distance between two PSSs in the same unit is set to be 1mm which is the accuracy achievable.

As shown in Fig. 2, a source laser is installed on the measurement frame of the moving component, and a PSD is mounted on the fixed component. The source laser transmits a horizontal light beam which is received by the PSD which can get the position deviation of light point from the center and then calculate the relative displacement errors between two assembling components along X and Z axis with high accuracy.

Generally, the task of automated assembly of two large-scale components can be treated as the process of posture adjustment of moving part with respect to the fixed part. The geometric model is established in the Cartesian coordinate system while the fixed coordinate system  $O_F-X_F Y_F Z_F$  is associated with the fixed component, and the measuring coordinate system  $O_M-X_M Y_M Z_M$  is fixed on the moving component.

Instead of establishing a transformation relationship between the fixed coordinate system  $O_F-X_F Y_F Z_F$  and the measuring coordinate  $O_M-X_M Y_M Z_M$ , the measurement procedure is actualized step by step. As shown in Fig. 3, the procedure can be divided into the following steps:

**Phase 1 Leveling:** Rotate the moving part around  $X_F$  and  $Y_F$  axes respectively through the 3-DOF redundant manipulator with the measurement data from the tilt sensors, until the plane  $X_F O_F Y_F$  is parallel to the coordinate plane  $X_M O_M Y_M$ .

**Phase 2 Pre-Adjustment in Z:** Make the moving part translate along the  $Z_M$ -axis through the 3-DOF redundant

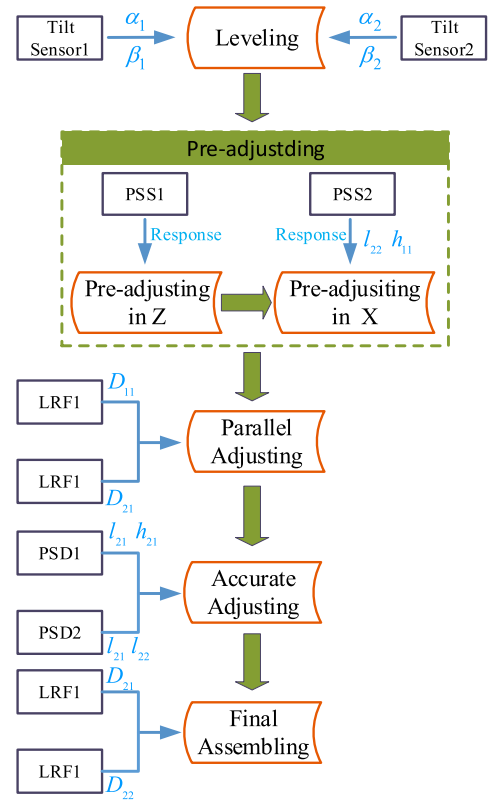


FIGURE 3. Adjustment steps.

manipulator, until the two return values from PSS unit are on and off.

**Phase 3 Pre-Adjustment in X:** Make the moving part translate along the  $X_M$ -axis through the 3-DOF planar manipulator, until the two return values from PSS unit b are on and off.

**Phase 4 Parallel Adjustment:** Rotate the moving part around the  $Z_M$ -axis through the planar rotation stage with the feedback of two LRFs, until the plane  $X_F O_F Z_F$  is parallel to the coordinate plane  $X_M O_M Z_M$ .

**Phase 5 Accurate Adjustment:** Make the moving part translate along the  $X_F$ -axis and  $Z_F$ -axis through the 3-DOF planar manipulator according to deviations from PSDs.

**Phase 6 Final Assembling:** After the final alignment of two assembling components is achieved, translate the moving component along the  $Y_F$  axis to complete the assembly process.

### III. MATHEMATIC MODEL FOR EACH ASSEMBLY PHASE

#### A. LEVELING ADJUSTMENT

Firstly, the adjusting mechanism makes adjustment according to the moving the inclination angles  $\alpha$  and  $\beta$  around axis  $X_M$  and  $Y_M$  relative to the horizontal plane from the tilt sensors. As shown in fig. 4, coordinate  $O_M-X_M Y_M Z_M$  transfers into coordinate  $O_1-X_1 Y_1 Z_1$  which is parallel to the horizontal plane eventually.

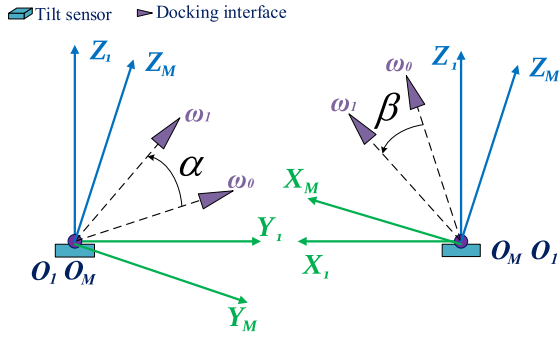


FIGURE 4. Leveling adjustment model.

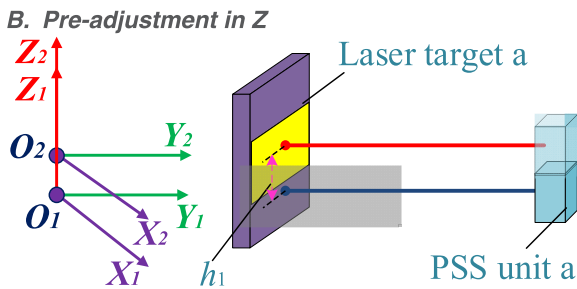


FIGURE 5. Pre-adjustment model in Z.

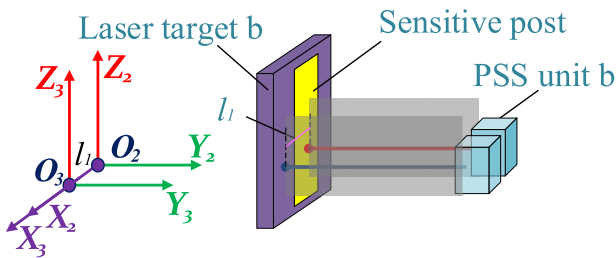


FIGURE 6. Pre-adjustment model in X.

Assume that vector  $w_0 = [X_F \ Y_F \ Z_F]^T$  is the coordinates of docking interface in  $O_M-X_M Y_M Z_M$  and vector  $w_1 = [X_L \ Y_L \ Z_L]^T$  is the coordinates in  $O_1-X_1 Y_1 Z_1$ . Then the transformation of the coordinates of docking interface can be expressed as follow:

$$\begin{aligned} \begin{bmatrix} X_L \\ Y_L \\ Z_L \end{bmatrix} &= \begin{bmatrix} c_\beta & s_\beta \\ -s_\beta & c_\beta \end{bmatrix} \begin{bmatrix} 1 & c_\alpha & -s_\alpha \\ & s_\alpha & c_\alpha \end{bmatrix} \begin{bmatrix} X_F \\ Y_F \\ Z_F \end{bmatrix} \\ &= \begin{bmatrix} c_\beta & s_\alpha s_\beta & c_\alpha s_\beta \\ 0 & c_\alpha & -s_\alpha \\ -s_\beta & s_\alpha c_\beta & c_\alpha c_\beta \end{bmatrix} \begin{bmatrix} X_F \\ Y_F \\ Z_F \end{bmatrix} \end{aligned} \quad (1)$$

### B. PRE-ADJUSTMENT IN Z

As illustrated in Fig. 2, two PSS units are installed on the ends of the fixed component. There are two light beams with specific distance from each PSS unit and each laser beam will forms a spot on the reflector. A sensitive reflector is glued on the target, if the light spot of PSS is shot within the sensitive post, the feedback of PSS is 1, otherwise it will feedback 0. The mechanism makes the moving part translate along

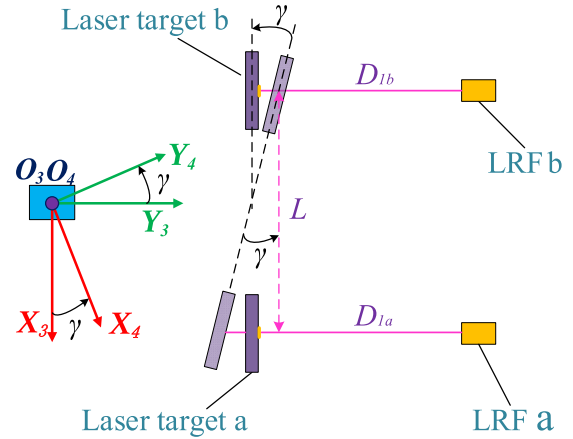


FIGURE 7. Parallel adjustment model.

axis- $Z_1$  until two beams ride just on two side of the reflector's edge on the target, while feedbacks of PSSs are 1 and 0. In this progress, coordinate  $O_1-X_1 Y_1 Z_1$  transfers into coordinate  $O_2-X_2 Y_2 Z_2$ .

### C. PRE-ADJUSTMENT IN X

Similarly to pre-adjustment in Z, we also use a PSS unit installed vertically to PSS unit a. As is shown in Fig. 6, the coordinate  $O_2-X_2 Y_2 Z_2$  transfers into coordinate  $O_3-X_3 Y_3 Z_3$ .

Suppose that the distance of translation in phase B is  $h_1$  and that in phase C is  $l_1$ , then the transformation of the coordinates between  $O_1-X_1 Y_1 Z_1$  and  $O_3-X_3 Y_3 Z_3$  can be expressed as follow:

$$\begin{bmatrix} X_R \\ Y_R \\ Z_R \end{bmatrix} = \begin{bmatrix} l_1 \\ 0 \\ h_1 \end{bmatrix} + \begin{bmatrix} X_L \\ Y_L \\ Z_L \end{bmatrix} \quad (2)$$

### D. PARALLEL ADJUSTMENT

In this phase, the moving part is made parallel with the fixed part on the base of the rotation error in  $Z_M$ -axis. We install two LRFs along the  $Y_M$ -axis. The distance between LRF a and LRF b is  $L$ . Use the laser targets to reflect laser signal, and get each distance  $D_{1a}$  and  $D_{1b}$ .

As shown in Fig. 7, the rotation error between the components is  $\arctan(D_{1a}-D_{1b})/L$ . Rotate around the axis  $Z_3$  at angle  $\gamma$  until it equals  $\arctan(D_{1a}-D_{1b})/L$ . then the transformation of the coordinates between  $O_3-X_3 Y_3 Z_3$  and  $O_4-X_4 Y_4 Z_4$  can be expressed as follow:

$$\begin{bmatrix} X_P \\ Y_P \\ Z_P \end{bmatrix} = \begin{bmatrix} c_\gamma & -s_\gamma \\ s_\gamma & c_\gamma \\ & & 1 \end{bmatrix} \begin{bmatrix} X_R \\ Y_R \\ Z_R \end{bmatrix} \quad (3)$$

In which  $\gamma = \arctan(D_1 - D_2) / L$ .

### E. ACCURATE ADJUSTMENT

After the rough adjustment mentioned above, the deviation between the moving part and fixed part is narrowed to a smaller range, and we can use two PSDs, with smaller range and higher accuracy, to obtain the relatively deviation.

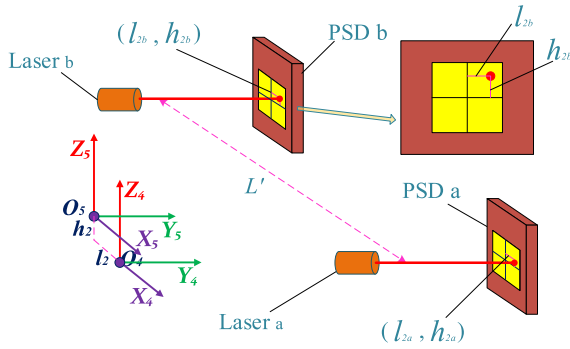


FIGURE 8. Accurate adjustment model.

There are two PSD sensors setting on the edge of the fixed part. The laser from the laser generator is received by PSDs which will give the deviations,  $l_{2a}$  and  $l_{2b}$  in  $X_4$ -axis, then  $h_{2a}$  and  $h_{2b}$  in  $Z_4$ -axis. As shown in Fig. 8,  $(l_{2a}, h_{2a})$  and  $(l_{2b}, h_{2b})$  are the values from PSD a and PSD b respectively. If  $l_2 = (l_{2a} + l_{2b})/2$  and  $h_2 = (h_{2a} + h_{2b})/2$ , the transformation of the coordinates between  $O_4$ - $X_4Y_4Z_4$  and  $O_5$ - $X_5Y_5Z_5$  can be expressed as follow:

$$\begin{bmatrix} X_A \\ Y_A \\ Z_A \end{bmatrix} = \begin{bmatrix} l_2 \\ 0 \\ h_2 \end{bmatrix} + \begin{bmatrix} X_P \\ Y_P \\ Z_P \end{bmatrix} \quad (4)$$

**F. FINAL ADJUSTMENT**

In this phase, there is only deviation in  $Y_M$ -axis. The two LRFs mentioned above can measure the distance in  $Y_M$ -axis. Setting  $D_{2a}$  and  $D_{2b}$  as the distances between two assembling components in  $Y_M$  direction measured by LRF a and LRF b respectively. Move the moving part over a distance of  $d_2$  along the  $Y$ -axis direction until it satisfies the relation:  $d_2 = (D_{2a} + D_{2b})/2$ . Then the assembly process is completed and the transformation of the coordinates between  $O_5$ - $X_5Y_5Z_5$  and  $O_6$ - $X_6Y_6Z_6$  can be expressed as follow:

$$\begin{bmatrix} X_D \\ Y_D \\ Z_D \end{bmatrix} = \begin{bmatrix} 0 \\ d_1 \\ 0 \end{bmatrix} + \begin{bmatrix} X_A \\ Y_A \\ Z_A \end{bmatrix} \quad (5)$$

Through the transformation of each adjustment phase, the coordinates of docking interface have changed from  $(X_M, Y_M, Z_M)$  to  $(X_F, Y_F, Z_F)$ ,

Suppose that

$$\begin{bmatrix} X_M & Y_M & Z_M & 1 \end{bmatrix}^T = T \begin{bmatrix} X_F & Y_F & Z_F & 1 \end{bmatrix}^T \quad (6)$$

The transformation can be calculated as follow (7), as shown at the bottom of the next page:

**IV. APPLICATION**

**A. DESCRIPTION OF THE PROTOTYPE**

Recently we have carried out a research project for automated assembly of mobile radar antennas in outdoor environment. The goal of this project is to apply automated assembly

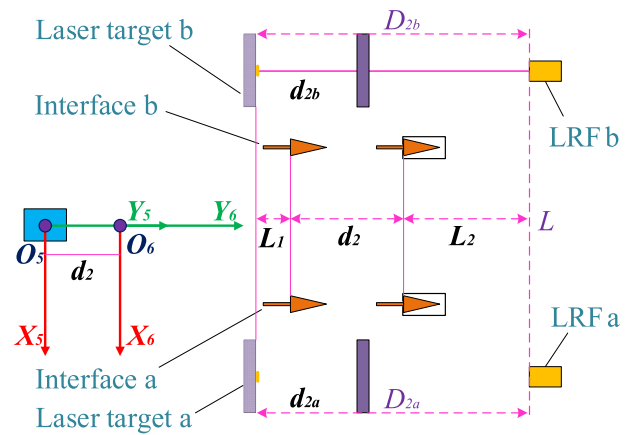


FIGURE 9. Final assembly model.

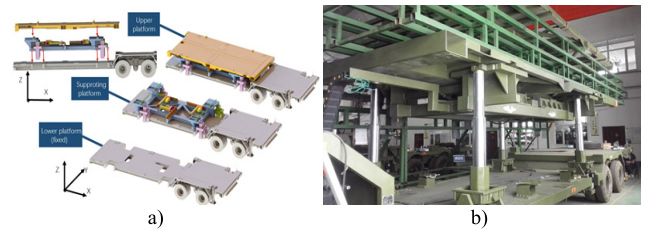


FIGURE 10. Graphic model of automated assembly system. a) 3D model of the novel mechanism. b) Physical device in operation.

techniques and digital measurement to the assembly of large-scale radars, which is crucial for enlarging antenna arrays and improving the mobility of vehicle-borne radars.

The automated assembly system consists of a posture alignment system installed on a vehicle, and a digital measurement system between components. The architecture of the posture alignment system is defined by a three-layer scheme to obtain a compact and symmetrical design. We developed a novel compact mechanism for a long travel range in automated assembly adjustment. This new mechanism, comprising a vehicle base, an inferior support base and a moving central platform, is shown in Fig. 10. As depicted, the moving platform is installed on the inferior plate. The whole size of the complex system is approx. 12 m × 2.50 m in the footprint, and approx. 0.7m in height. In addition, the use of three different layers effectively reduce the total height.

**B. SET-UP OF THE VERIFICATION SYSTEM**

The proposed large-scale measuring system has been tested on the radar antenna automated assembly system. We have designed a simulated antenna frame as the moving part fixed on the manipulator. As shown in Fig. 11, the fixed antenna has been designed as a frame structure to provide necessary installation of measurement target. To simplify the experiment system and meet the requirement of measuring system validation, we designed a pair of pin-hole parts on two assembly connection interface to verify the automated assembly results. If the center of hole of two pin-hole parts is aligned, the accuracy of automated assembly is success.

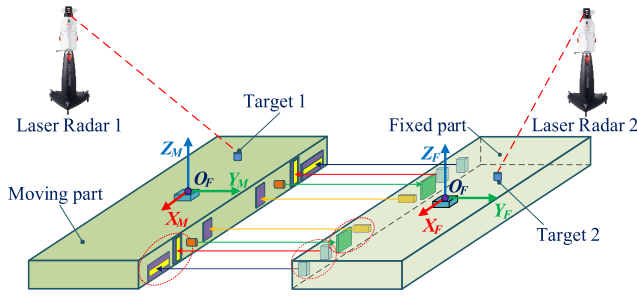


FIGURE 11. Photograph of experiment system.

At the same time, we set two laser radars fixed on the ground and two targets on each component to track the more accurate position.

The system mainly consists of three modules, as shown in Fig. 12. The sensor system is composed of two PSSs (type: BANNER QS18VP6LLP, range: 10m, response time: 700us, repeatability: 130us), lasers, two tilt sensors (type: Witlink AIS2000, angle accuracy: 0.002°, resolution: 0.0005°), two LRFs (type: SENSOPART FT80RLA 5000S1L8, range: 500mm, resolution: 0.1mm; light: 650nm) and two PSDs (type: hasunopto HS-2DPSD, Resolution: 3um, accuracy: 5um) which send position information to the CPU (Siemens PLC: S7-300) through RS485. A touchscreen is used to display the state of the assembly system. When the task start, the CPU firstly carries out position analysis according to the data input from the sensor system and determine if the task has been done. If done, which means the relative pose obtained from the data input meets the assembly requirements, the task should be discontinued. Otherwise, the trajectory will derive the time trajectories of the desired task space position, velocity and acceleration vectors (which are considered reference vectors for the manipulator system).

The manipulator system block is composed of four sub-blocks. The Jacobian matrix transpose block gives the actual joint space input vector of the manipulator using its task space state input vector obtained from the CPU. The actuator block provides the actual inputs to the mechanical structure. The mechanical structure mainly consists of servo motors and mechanism structures. This dynamic system adopts PID control method by placing the PID controller block in the manipulator system. The sensor system keeps obtaining pose information after the manipulator finish a round of adjustment until the CPU determine to stop the task.

### C. PROCEDURES AND RESULTS

Based on calibration for the laser sensors and corresponding targets, the preliminary measurement and automated

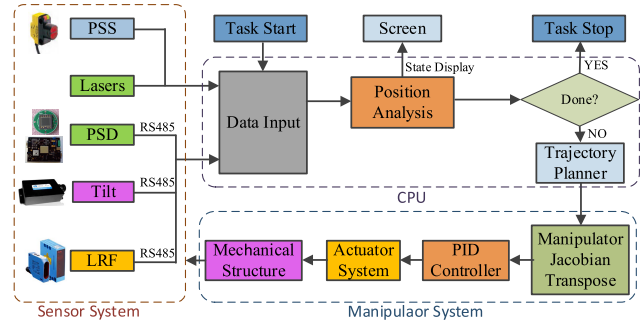


FIGURE 12. Photograph of control strategy.

assembly experiments are carried out. The tests mainly focus on the precision of the automated large-scale measurement system.

#### 1) ROUGH ALIGNMENT EXPERIMENT

In the experiments, the posture deviation between the fixed frame structure and the simulate antenna is set to be about 200mm,400mm,200 mm in X, Y, Z axis respectively, and the pitch angle of the moving part is set to be about 1.5°.

Fig. 13 illustrates the automated assembly process. Firstly, the target position of assembling antenna is calibration. This can be realized by driving the posture adjustment mechanism manually, by using hand control box to move the simulation antenna at assembly mating position with fixed frame structure. The accurate position of assembling antenna is measured with Laser tracker. Then each chain of the posture adjustment system is reset to its initial position, as shown in Fig. 13. (a). After that, the automated assembly operation starts. First, as shown in Fig. 13. (b), the rough adjusting operation is carried out. Four leg-lifting mechanisms and planar 3-DOF PM are successively actuated to search the target and reduce the pose and distance deviation between two assembled parts. After that, the second and third linear actuators are actuated to keep the assembling antenna parallel with the fixed frame with the two LRFs. In this stage, we can see the posture of assembling antenna is adjusted near to the fixed frame, and the light spots of all laser sensors are in corresponding targets. It can be seen that the light spots are very close to their target position. After rough alignment phase, the pose adjustment operation can be advanced at a slower rate to approach the assembling position. As shown in Fig. 13. (c), this operation is finished until all the laser sensors' feedback have reached the threshold requirements. Finally, moving the assembling antenna to approach the fixed frame along Y axis, according to the distance measured by LRFs. The overall

$$T = \begin{bmatrix} R_\gamma R & P \\ 0 & 1 \end{bmatrix} = \begin{bmatrix} c_\beta c_\gamma & s_\alpha s_\beta c_\gamma - c_\alpha s_\gamma & c_\alpha s_\beta c_\gamma + s_\alpha s_\gamma & l_1 c_\gamma + l_2 + X_V \\ c_\beta s_\gamma & s_\alpha s_\beta s_\gamma + c_\alpha c_\gamma & c_\alpha s_\beta s_\gamma - s_\alpha c_\gamma & l_1 s_\gamma + d_1 + Y_V \\ -s_\beta & s_\alpha c_\beta & c_\alpha c_\beta & h_1 + h_2 + Z_V \\ 0 & 0 & 0 & 1 \end{bmatrix} \quad (7)$$

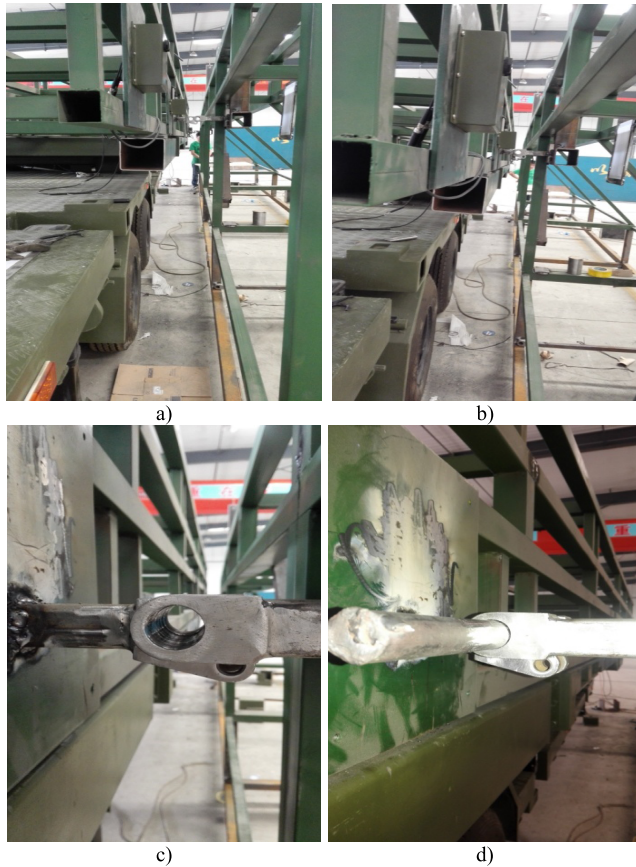


**FIGURE 13.** The process of automated assembly experiment. a) Initial position. b) After rough alignment. c) After accurate alignment. d) Assembly process completed.

process of automated assembly is finally completed, as shown in Fig. 13. (d).

The entire rough alignment process is automatically performed. The measurement and adjustment errors in this stage are observed with the feedbacks of two PSD sensors and LRFs. After repeating the experiments 10 times, we record the position and orientation errors between the moving part and the fixed part after the whole adjustment process is completed. The final test data is shown in TABLE I.

The errors in assembly alignment for each condition at different initial distances are depicted in Fig. 14. As summarized in Fig. 14, the distance errors at each experiment shows that the positioning errors of the system is about 2 mm and the reproducibility is less than 1 mm. The maximum deviations are 1.98 mm and 1.90 mm in Fig. 14(a) and (b), respectively. The errors are probably occurred due to the fabrication and installation of the calibration device, and the frame vibration during the assembly operation.

2) ACCURATE ALIGNMENT EXPERIMENT

In the accurate alignment process, we use the PSD sensor to obtain the required measurement information. The laser tracker is applied to monitor 6 DOFs of an object with high accuracy over large range. In order to evaluate the measuring

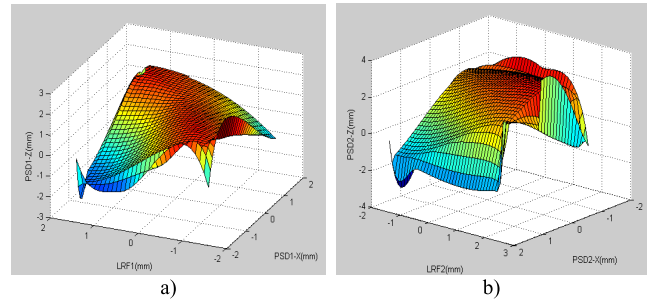


**FIGURE 14.** The errors of automated assembly experiment after rough alignment operation. a) Errors of the left side. b) Errors of the right side.

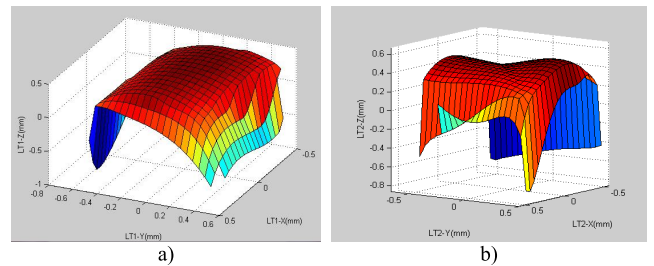


**FIGURE 15.** The errors of automated assembly experiment after accurate alignment operation. a) Errors of the left side. b) Errors of the right side.

accuracy of the measurement system in the radar antenna automated assembly system, an experiment is carried out with the respective monitoring of laser trackers.

During the experiment, the fixed test frame is stationary and the target assembly position and orientation of moving part is fixed. Therefore, we can evaluate the overall accuracy of proposed measurement system by measuring the final position with laser tracker after fine alignment operation. A total number of 10 experiments with different initial positions and orientations for automatic assembly operation were conducted for evaluation. Relevant test data is shown in TABLE I.

The deviations in 10 positions and orientations of the verification experiment are plotted in Fig. 15. It is obviously that the proposed method has achieved good performance in this task by accuracy. The maximum positioning error is about 0.5 mm and can meet the requirement of large radar antenna automated assembly.

3) DISCUSSION

The experiments and analysis above show that, in rough alignment stage, the measurement system can guide the moving antenna to reduce its posture deviation with fixed antenna. By analyzing the measurement errors of the experiments, a measurement accuracy of 2mm is achieved. This precision ensures the light spot emitted by the PSD sensor cannot reach the target, and then the accurate adjustment phase can be started. Still, a measurement accuracy of 0.5mm is achieved through the control of posture alignment mechanism with the feedback of PSD sensors, which guarantee proper alignment of two assembling radar antennas. However, from

TABLE 1. Experimental data of adjustment operation.

No.	Before adjustment(mm)				After rough adjustment operation (mm)						After accurate adjustment operation (mm)					
	$\Delta x$	$\Delta X$	$\Delta X$	$\alpha$	LRF1	LRF2	PSD1-X	PSD1-Z	PSD2-X	PSD2-Z	LRF1	LRF2	PSD1-X	PSD1-Z	PSD2-X	PSD2-Z
1	200	500	100	1.5°	281.45	281.96	1.85	1.31	-1.21	-0.91	0.483	-0.497	0.217	0.491	-0.512	0.227
2	300	500	100	1.5°	281.53	281.70	-1.90	1.29	0.86	1.57	-0.389	0.586	-0.782	-0.454	-0.499	-0.776
3	200	500	200	2°	281.51	278.09	1.81	-1.47	-1.23	1.62	-0.381	-0.415	0.203	0.468	-0.507	-0.786
4	300	500	200	2°	281.49	281.97	-1.7	-1.37	1.56	-1.91	-0.489	-0.576	-0.596	-0.407	0.507	0.215
5	300	500	300	2°	281.56	278.17	1.77	1.46	1.48	-1.47	0.397	-0.507	-0.856	0.456	0.479	-0.801
6	200	300	100	1.5°	278.63	281.78	-1.61	1.35	-1.32	1.56	-0.476	0.498	0.226	-0.407	-0.511	0.302
7	300	300	100	1.5°	278.50	278.02	1.70	-1.03	1.56	1.64	0.305	0.318	0.205	0.451	0.438	0.221
8	200	300	200	2°	278.43	278.04	-1.86	-1.32	-1.53	-1.78	0.454	0.547	-0.793	0.538	0.510	-0.746
9	300	300	200	2°	280.26	282.17	0.85	1.25	-1.49	-1.61	0.399	-0.479	0.203	-0.469	0.502	-0.776
10	300	300	300	2°	281.27	282.05	0.95	1.36	1.45	1.96	0.475	-0.507	0.214	0.413	-0.499	0.297

the experiment results, we can note that the errors around the X axis is relatively higher than other directions. It is because of the measurement accuracy depends only on the tilt sensor. Considering that the size of assembling antennas in Y direction is relatively small, the angle error in this direction is within the scope of assembly accuracy.

Overall, the developed measurement system provides a low-cost and high-accuracy solution for measurement tasks in automated assembly of large scale radar antennas. The measurement system consists of laser sensors and is insensitive to fog, rain, and sunlight in outdoor environment. Our test system has achieved good results and this show that the proposed measuring system is feasible.

Similar to the above experimental device, when designing the assembly components, we are supposed to design the mounting position of the sensors, when installing the sensors, we are supposed to put the moving component in the target position, then set the sensors' output value to zero. After doing this, we can start the process of assembly. The position of the sensors is fixed, and after putting the system into use, we can't move the sensors. Before the next docking process, we needn't to re-calibrate the sensors. That is to say, in the whole life cycle of the measurement and docking system, we just need to calibrate the sensors for only once.

## V. CONCLUSION

This paper presents a large-scale 3D measurement system for automated assembly of large size products. Combination of low-cost tilt sensor and laser sensors is used for measurement. The system construction and measurement principle are introduced specifically. Subsequently, the geometric measurement model for each assembly stage is established. The characteristics of this measurement technology is dividing the whole measuring process into 6 major alignment phases to complete the automated assembly task. A prototype system for assembling two large radar antennas automatically is established to validate proposed large-scale measuring technology. Various experiments are preformed and the results demonstrated that proposed measurement system has

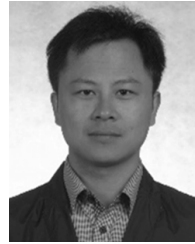
absolute accuracy about (+/- 0.5mm) for the positioning of large antenna arrays (approximately 12m × 2.5m). The experiment results definitely proved that the proposed measurement system is feasible and has good accuracy, and therefore is suitable for the position measurement in large-scale automated assembly system. Future work will be focused on developing a self-adaption planning and data processing method to speed up the measuring process and improve the performance in outdoor environment, thus improving system efficiency and measuring accuracy as well.

## REFERENCES

- [1] Y. Gao, J. Lin, L. Yang, and J. Zhu, "Development and calibration of an accurate 6-degree-of-freedom measurement system with total station," *Meas. Sci. Technol.*, vol. 27, no. 12, p. 125103, 2016.
- [2] F. Franceschini, M. Galetto, D. Maisano, and L. Mastrogiacomo, "Large-scale dimensional metrology (LSDM): From tapes and theodolites to multi-sensor systems," *Int. J. Precis. Eng. Manuf.*, vol. 15, no. 8, pp. 1739–1758, 2014.
- [3] J. DeLand, "Large scale assembly utilizing laser radar & IRGPS," SAE Tech. Paper 2004-01-2831, 2004.
- [4] G. X. Zhang, J. W. Yao, Z. R. Qiu, W. C. Hu, F. Z. Fang, and X. H. Li, "Large-scale space angle measurement," *CIRP Ann.*, vol. 57, no. 1, pp. 525–528, 2008.
- [5] J. H. Zou et al., "The iGPS measurement technology application for the aircraft flexible joint assembly," SAE Tech. Paper 10AMAF-0015, 2010.
- [6] G. Mosqueira, J. Apetz, K. M. Santos, E. Villani, R. Suterio, and L. G. Trabasso, "Analysis of the indoor GPS system as feedback for the robotic alignment of fuselages using laser radar measurements as comparison," *Robot. Comput.-Integr. Manuf.*, vol. 28, no. 6, pp. 700–709, 2012.
- [7] Z. Liu, J. Zhu, L. Yang, H. Liu, J. Wu, and B. Xue, "A single-station multi-tasking 3D coordinate measurement method for large-scale metrology based on rotary-laser scanning," *Meas. Sci. Technol.*, vol. 24, no. 10, p. 105004, 2013.
- [8] W. Cuyppers, N. Van Gestel, A. Voet, J.-P. Kruth, J. Mingneau, and P. Bleys, "Optical measurement techniques for mobile and large-scale dimensional metrology," *Opt. Lasers Eng.*, vol. 47, nos. 3–4, pp. 292–300, 2009.
- [9] R. H. Schmitt et al., "Advances in large-scale metrology—Review and future trends," *CIRP Ann.*, vol. 65, no. 2, pp. 643–665, 2016.
- [10] H. Ukai, K. Nakamura, and N. Matsui, "DSP- and GPS-based synchronized measurement system of harmonics in wide-area distribution system," *IEEE Trans. Ind. Electron.*, vol. 50, no. 6, pp. 1159–1164, Dec. 2003.
- [11] R. Mautz, "Overview of current indoor positioning systems," *Geodesy Cartogr.*, vol. 35, no. 1, pp. 18–22, 2009.
- [12] H. Liu, H. Darabi, P. Banerjee, and J. Liu, "Survey of wireless indoor positioning techniques and systems," *IEEE Trans. Syst., Man, Cybern. C, Appl. Rev.*, vol. 37, no. 6, pp. 1067–1080, Nov. 2007.



- [13] Z. Guo, J. Jiang, and Y. Ke, "Stiffness of postural alignment system based on 3-axis actuators for large aircraft components," *Chin. J. Mech. Eng.*, vol. 23, no. 4, pp. 524–531, 2010.
- [14] Z. Wang, L. Mastrogiacomo, F. Franceschini, and P. Maropoulos, "Experimental comparison of dynamic tracking performance of iGPS and laser tracker," *Int. J. Adv. Manuf. Technol.*, vol. 56, nos. 1–4, pp. 205–213, 2011.
- [15] W. T. Estler, K. L. Edmundson, G. N. Peggs, and D. H. Parker, "Large-scale metrology—An update," *CIRP Ann.*, vol. 51, no. 2, pp. 587–609, 2002.
- [16] Z. Chen, F. Du, and X. Tang, "Position and orientation best-fitting based on deterministic theory during large scale assembly," *J. Intell. Manuf.*, vol. 29, no. 4, pp. 827–837, 2015.
- [17] W.-F. Xie, Z. Li, X.-W. Tu, and C. Perron, "Switching control of image-based visual servoing with laser pointer in robotic manufacturing systems," *IEEE Trans. Ind. Electron.*, vol. 56, no. 2, pp. 520–529, Feb. 2009.
- [18] P. Wang *et al.*, "Robotic assembly system guided by multiple vision and laser sensors for large scale components," in *Proc. IEEE Int. Conf. Robot. Biomimetics (ROBIO)*, Dec. 2015, pp. 1735–1740.
- [19] H.-L. Hsieh and S.-W. Pan, "Development of a grating-based interferometer for six-degree-of-freedom displacement and angle measurements," *Opt. Express*, vol. 23, no. 3, pp. 2451–2465, 2015.
- [20] B. Chen, B. Xu, L. Yan, E. Zhang, and Y. Liu, "Laser straightness interferometer system with rotational error compensation and simultaneous measurement of six degrees of freedom error parameters," *Opt. Express*, vol. 23, no. 7, pp. 9052–9073, 2015.
- [21] C.-Y. Chang and H. W. Lie, "Real-time visual tracking and measurement to control fast dynamics of overhead cranes," *IEEE Trans. Ind. Electron.*, vol. 59, no. 3, pp. 1640–1649, Mar. 2012.
- [22] S. Zhu and Y. Gao, "Noncontact 3-D coordinate measurement of cross-cutting feature points on the surface of a large-scale workpiece based on the machine vision method," *IEEE Trans. Instrum. Meas.*, vol. 59, no. 7, pp. 1874–1887, Jul. 2010.
- [23] X. Zhang *et al.*, "A universal and flexible theodolite-camera system for making accurate measurements over large volumes," *Opt. Lasers Eng.*, vol. 50, no. 11, pp. 1611–1620, 2012.
- [24] Y. Gao, J. Lin, F. He, S. Yin, and J. Zhu, "A monocular vision and inclinometer combined system for 6DOF measurement of double shield TBM," *Sens. Actuators A, Phys.*, vol. 249, pp. 155–162, Oct. 2016.
- [25] L. Qi, X. Zhang, J. Wang, Y. Zhang, S. Wang, and F. Zhu, "Error analysis and system implementation for structured light stereo vision 3D geometric detection in large scale condition," *Proc. SPIE*, vol. 8555, pp. 855521-1–855521-8, Nov. 2012.
- [26] J. Wu, J. Zhu, Z. Yu, J. Zhuge, and B. Xue, "A total station spatial positioning method based on rotary laser scanning and ultrasonic ranging," *Rev. Sci. Instrum.*, vol. 87, no. 11, p. 115104, 2016.
- [27] M. Grosse-Schwiep, J. Piechel, and T. Luhmann, "Measurement of rotor blade deformations of wind energy converters with laser scanners," *J. Phys., Conf. Ser.*, vol. 524, no. 1, p. 012067, 2014.
- [28] Y.-K. Kim *et al.*, "Developing accurate long-distance 6-DOF motion detection with one-dimensional laser sensors: Three-beam detection system," *IEEE Trans. Ind. Electron.*, vol. 60, no. 8, pp. 3386–3395, Aug. 2013.
- [29] X. Yu, S. R. Gillmer, S. C. Woody, and J. D. Ellis, "Development of a compact, fiber-coupled, six degree-of-freedom measurement system for precision linear stage metrology," *Rev. Sci. Instrum.*, vol. 87, no. 6, p. 065109, 2016.



**GAOLIANG PENG** received the B.S., M.S., and Ph.D. degrees in mechanical engineering from the Harbin Institute of Technology in 2001, 2003, and 2007, respectively. He held a post-doctoral position at the Department of Computer Science, Harbin Institute of Technology.

He is currently an Associate Professor and the Director of the Faculty of Mechatronics and Automation. His research interests include CAD/CAM, robotic servo control, and automatic assembly of mobile radar antenna.



**YU SUN** received the B.S. and M.S. degrees in mechanical engineering from the Harbin Institute of Technology in 2014, and 2016, respectively, where he is currently pursuing the Ph.D. degree in mechanical engineering.

His research interests include kinematics, dynamics and control of parallel kinematic machine, and optimal design of redundant parallel mechanisms.



**SHILONG XU** received the B.S. degree in mechanical engineering from the Harbin Institute of Technology in 2017, where he is currently pursuing the M.S. degree in mechanical engineering.

His research interests include position and orientation measurement, sensor arrays, and structural health monitoring.

• • •